Comparison of Remeshing and Material Point Method Approaches for Large-Strain Assessment of a Tailings Storage Facility Under Residual Undrained Strength Conditions

Myzael Valdivia, Klohn Crippen Berger, Canada
Miguel Regalado, Klohn Crippen Berger, UK
Vicki Nguyen, Klohn Crippen Berger, Canada

Abstract

Recent tailings storage facility (TSF) failures have demonstrated the importance of brittle strain-weakening and static liquefaction mechanisms in controlling instability and large deformations. The 2014 Mount Polley failure involved brittle strain-weakening of a foundation layer that led to progressive failure, while the 2018 Cadia failure involved weakening of a foundation layer that triggered static liquefaction of stored tailings and subsequent displacement of the embankment. These case histories demonstrate that understanding deformation patterns associated with residual strength mobilization is essential for risk-informed TSF management.

Remediation measures intended to achieve the limit equilibrium (LE) stability factors of safety (FoS) recommended by guidelines may be constrained by downstream infrastructure or lease boundaries and may therefore be unable to fully satisfy the design criteria. In such cases, the assessment of the expected deformation response and post-trigger behavior may provide a more appropriate framework for assessing system performance than reliance on LE FoS values alone.

This paper presents a comparative large-strain deformation assessment of an upstream TSF section with a downstream buttress under residual undrained conditions. A representative interim buttress geometry incorporating a bench and a shear key is analyzed assuming direct mobilization of residual undrained strengths within the contractive tailings and foundation materials. Two large-strain numerical approaches available within FLAC2D are evaluated: automatic remeshing and the Material Point Method (MPM) (MPoint2D module).

The results indicate significant differences between the remeshing and MPM simulations with respect to the magnitudes of the predicted displacements. The analyses also demonstrate a significant sensitivity to mesh and material point discretization, even when simplified constitutive representations are adopted. The

configuration with full shear key penetration exhibited substantially shorter runout distances than the configurations with partial or no shear key penetration.

Introduction

Recent tailings storage facility (TSF) failures have demonstrated the importance of brittle strain-weakening and static liquefaction mechanisms in controlling instability and large deformations. The 2014 Mount Polley failure involved progressive failure initiated within a weak glaciolacustrine foundation layer, while the 2018 Cadia failure involved weakening of a foundation layer that triggered static liquefaction of stored tailings and subsequent displacement of the embankment. These case histories highlight that evaluating only conventional stability conditions may not be sufficient to characterize TSF performance, particularly when large deformations may develop following residual strength mobilization.

Numerical modelling of strain-weakening systems presents important challenges associated with mesh sensitivity and strain localization. Zabolotnii et al. (2021) demonstrated that numerical analyses of strain-weakening materials are highly dependent on mesh discretization because conventional continuum formulations cannot explicitly represent the very thin shear bands that develop during localization. Under these conditions, progressively refined meshes may produce more realistic results and increasingly localized deformation patterns. The study further showed that lower-bound responses may be represented through simplified “instant weakening” approaches in which materials transition directly from peak to residual conditions. From an engineering perspective, residual undrained strength analyses may therefore provide a practical framework for evaluating post-localization response in TSFs where the thickness and evolution of shear bands cannot be represented explicitly with confidence.

Given that residual undrained strength mobilization may result in large deformations and post-failure runout, conventional small-strain numerical approaches may become insufficient to characterize system response. In recent years, large-strain numerical methods such as MPM have gained increasing attention in geotechnical engineering because of their ability to simulate large deformations without the mesh distortion limitations associated with traditional finite-difference or finite-element formulations. Applications have expanded to landslides, static liquefaction problems, and tailings dam breach analyses (Lino et al., 2025). More recently, large-strain capabilities such as automatic remeshing (Itasca, 2026a) and MPM (MPoint2D module) (Itasca, 2026b) formulations have been incorporated into FLAC2D, allowing practitioners to evaluate large deformation problems using numerical approaches specifically developed to address severe mesh distortion and post-failure material movement. These developments provide new opportunities for deformation-based assessment of TSFs under residual undrained strength conditions and motivate the comparison between different large-strain numerical approaches.

This paper presents a comparative large-strain assessment of an upstream TSF under residual undrained strength conditions using two numerical approaches available within FLAC2D: automatic remeshing and MPM. The study focuses on TSF embankment configuration constrained by operational conditions and evaluates the influence of the selected large-strain formulation on predicted deformation magnitude, runout distance, and overall failure mechanism development.

Theoretical Background

Large deformations associated with residual undrained strength mobilization may exceed the capabilities of conventional small-strain numerical formulations. In finite-difference and finite-element approaches, excessive distortion of computational zones may lead to loss of numerical stability, inability to complete the analysis, or unrealistic deformation patterns.

Recent developments in the FLAC2D software include large-strain capabilities based on automatic remeshing (Itasca, 2026a) and MPM (Itasca, 2026b). In large-strain finite-difference analyses, severe zone distortion may lead to illegal geometries in which numerical calculations can no longer continue. The automatic remeshing functionality is intended to address these limitations by automatically regenerating the computational mesh when geometry quality criteria are violated during model cycling. During the remeshing process, zone, grid point, and face information from the distorted mesh are preserved and interpolated onto the regenerated mesh, after which numerical cycling continues. The approach allows continuation of analyses after severe deformation develops while maintaining a continuum-based finite-difference representation of the system. Although the formulation remains mesh-dependent and repeated interpolation may introduce some numerical inaccuracies, the approach significantly extends the capability of conventional finite-difference analyses to simulate large deformations and post-failure responses.

The MPM was originally developed by Sulsky et al. (1994) as a hybrid Eulerian-Lagrangian numerical approach for large deformation analysis. The method uses a double discretization consisting of material points, which store state variables such as mass, stress, strain, density, and velocity, together with a computational background grid where the governing equations are solved (Itasca, 2026b). This formulation allows material deformation to be tracked using the material points while avoiding many of the mesh distortion limitations associated with traditional continuum-based methods. As a result, MPM is well suited for the simulation of large deformation and post-failure material behavior. Recent applications of MPM in geotechnical engineering have included slope failures, static liquefaction problems, and tailings dam breach analyses. Macedo et al. (2024) and Lino et al. (2025) provide case studies demonstrating the application of the MPM to TSFs and waste dumps.

Recent developments in FLAC2D 9.7 incorporate the MPM formulation in the MPoint2D module, which allows coupling between the conventional finite-difference method (FDM) and material-point

calculations within the same numerical framework (Itasca, 2026b). The implementation allows existing FLAC models and constitutive formulations to be extended into large-deformation analyses through adaptive conversion of distorted finite-difference zones into material points while preserving material properties and state variables. This provides a practical workflow for evaluating post-failure deformation processes using models initially developed within a conventional FLAC environment.

In this study, both automatic remeshing and MPoint2D approaches available within FLAC are used to evaluate the deformation response of an upstream TSF under residual undrained strength conditions. The analyses compare predicted deformation magnitudes and overall failure mechanism evolution between the two large-strain approaches.

Example Study: Upstream TSF with a Rockfill Buttress

TSF Geometry

The foundation, tailings, and fill stratigraphy for this study, shown in Figure 1, represents a hypothetical scenario developed to investigate the model response under different analysis methodologies and shear key configurations. The model consists of an upstream tailings storage facility (TSF) and a two-stage downstream rockfill buttress located at the toe, with slopes of 4H:1V in the lower section and 6H:1V in the upper section, incorporating a shear key. The foundation profile comprises upper and lower clay layers, sandwiching a weak clay layer, underlain by till, and a continuous bedrock horizon at depth.

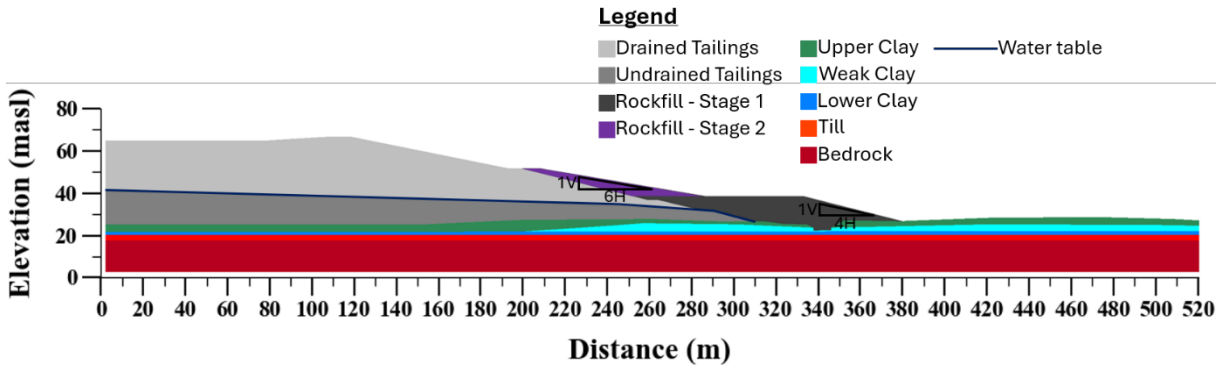


Figure 1: Tailings storage facility (partial shear key)

The weak clay layer represents the critical foundation unit controlling the deformation response of the system. The material is characterized as a sensitive foundation layer with low post-peak undrained shear resistance, conceptually analogous to weak foundation units involved in documented TSF failures such as Mount Polley and Cadia, where progressive foundation deformations contributed to instability development and triggering of static liquefaction within the overlying saturated tailings. To improve the global stability, the buttress includes a shear key intended to penetrate through the weak clay layer and transfer stresses into

the underlying competent foundation materials. Although the geometry and material properties used in this study do not correspond to a specific project, this example was developed to represent conditions commonly encountered in upstream TSFs founded on weak and strain-sensitive foundation materials.

Since the purpose of this model is to assess the post-trigger deformation response, residual undrained strengths were assigned directly at the beginning of the simulations rather than modelling potential triggering mechanisms explicitly. The analyses therefore follow a lower-bound residual-strength framework consistent with the concepts discussed by Zabolotnii et al. (2021). Residual undrained strengths were assigned to the weak clay and saturated tailings material to evaluate post-trigger response conditions for the TSF configuration, with the buttress designed for a factor of safety (FoS) equal to 1.

An additional uncertainty considered in the assessment was the possibility that the shear key did not fully penetrate the sensitive clay layer, resulting in the presence of an approximately 0.5 m thick weak clay layer beneath the shear key. Under these conditions, FoS became lower than 1, requiring large-strain analyses to evaluate potential deformation and runout distances. The assessment criterion considered that displacements should not extend beyond the assumed lease boundary, 7 m downstream of the toe.

The objective of the large-strain analyses presented in this study is therefore not to predict operational failures or triggering mechanisms, but to evaluate the potential magnitude and extent of deformations that could develop under a post-trigger residual-strength condition using different large-strain numerical formulations.

Model Parameters

Post-trigger large-strain analyses were performed using simplified constitutive representations under residual undrained strength conditions. The Mohr-Coulomb (MC) constitutive model was adopted for all materials within the large-strain simulations, except for the bedrock, which was represented using the Linear Elastic constitutive model. The MC model simulates soil behavior as linear elastic up to failure, which is controlled by the mobilized shear strength. Strength parameters were defined according to the expected drainage conditions. Effective stress parameters were assigned to drained materials, whereas undrained materials were modelled using undrained shear strength ratios corresponding to either peak or residual conditions.

Drained materials, including rockfill, drained tailings, till, and bedrock, were modelled using effective stress strength parameters. Weak clay and saturated tailings units were assigned residual undrained strength ratios to represent post-trigger conditions associated with brittle failure and static liquefaction mechanisms. The dilative (e.g. till and lower clay) foundation units were modelled using peak undrained strength ratios, while the upper clay was assigned an undrained strength equal to 80% of its peak value to represent slight brittle behavior. The selected parameters do not explicitly reproduce progressive strain-softening behavior;

instead, they provide a simplified representation of the residual strength response for the assessment of potential deformation consequences.

Table 1 summarizes the corresponding bulk and saturated density values. Bulk density values were assigned to materials located above the water table, whereas saturated density values were assigned to materials located below the water table. Material stiffness was derived by applying a reduction factor to the maximum shear modulus (G_{max}). A reduction factor of 3 was adopted to reflect the anticipated strain levels. The value of G_{max} was estimated from the soil mass density (ρ) and shear wave velocity (V_s) (Equation 1). Both G_{max} and V_s are stress-dependent and were evaluated using Equation 2 together with the normalized shear wave velocities (V_{s1}). Poisson's ratio and the initial stress ratio (K_0) were assumed to be 0.3 and 0.5, respectively. A summary of the adopted static material parameters is presented in Table 1.

$$G_{max} = \rho V_s^{\,2} \tag{1}$$

Where: G_{max}: Maximum shear modulus; ρ: Density; V_s: Shear wave velocity

$$V_s = V_{s1}\left(\frac{\sigma'_{v0}}{P_a}\right)^{m} \tag{2}$$

Where: V_{s1}: Shear wave velocity corrected to an effective overburden stress of 1 atm; σ'_{v0}: Initial vertical effective stress; P_a: Atmospheric pressure; m: Exponent.

Table 1: Summary of Main Parameters for the Large-Strain Analysis

Name	Bulk Unit Weight, γ_b (kg/m³)	Saturated Unit Weight, γ_{sat} (kg/m³)	Effective Friction Angle, ϕ' (°)	Peak Undrained Strength Ratio, S_{up}/σ_{v0}' (–)	Residual Undrained Strength Ratio, S_{ur}/σ_{v0}' (–)	V_{s1} (m/s)	m (–)
Rockfill	2,050	2,094.3	39	–	–	300	0.25
Drained Tailings	2,000	2,044.3	32	–	–	180	0.25
Undrained Tailings	2,000	2,044.3	–	–	0.1	180	0.25
Upper Clay	1,900	1,994.3	–	0.18	–	175	0.25
Weak Clay	1,900	1,994.3	–	–	0.1	175	0.25
Lower clay	1,900	1,994.3	–	0.22	–	175	0.25
Till	2,100	2,254.3	37	–	–	300	0.25
Bedrock	2,200	2,394.3	–	–	–	2,000	0

Large Strain Deformation Analysis

Numerical Model and Analysis Approach

The numerical modelling of the representative cross-section presented in Figure 1 was carried out using the finite-difference code FLAC2D 9.6.46 (Itasca, 2026a) for the conventional (small-strain and large-strain) and remeshing analyses and MPoint2D (embedded in FLAC2D 9.7.46) (Itasca, 2026b), for the MPM

analysis. The adopted modelling approach consisted of the initial static phase simulating staged TSF construction to establish in-situ stress conditions, followed by the stage aimed at evaluating post-trigger deformation behavior, numerical performance, and resulting runout distances.

The staged construction of the embankment was simulated under drained conditions using the MC constitutive model with effective strength parameters (not included in this paper), allowing the development of the effective stress distributions within the tailings, buttress, and foundation materials prior to the large-strain deformation analyses. During this stage, the analyses were performed using a small-strain calculation scheme.

Both small-strain and large-strain calculation schemes were evaluated using the finite-difference method (FDM) within a Lagrangian framework, with remeshing disabled. These approaches represent conventional practice in geotechnical numerical modelling and were included to provide a basis for comparison with the remeshing and MPoint2D formulations.

The spatial discretization of the model was defined to adequately represent stress gradients and deformation mechanisms, with mesh refinement in critical regions. Most of the model domain was discretized using elements with a characteristic size of approximately 0.5 m. A finer discretization was adopted in the shear key region, where the element size was reduced to approximately 0.25 m to improve the resolution of stress concentrations and potential shear localization. Above this region, a trapezoidal transition zone was implemented to provide a gradual change in element size between the refined mesh in the shear key and the coarser mesh in the upper portion of the model, thereby minimizing numerical artifacts associated with abrupt mesh transitions.

A second model was developed by refining the initial mesh horizontally and vertically by a factor of 2. Additional analyses considering configurations both with a fully penetrating shear key and without a shear key were also performed to establish reference upper- and lower-bound runout conditions. A comparison between the two mesh discretizations for the configuration including a 1 m thick weak clay beneath the shear key is presented in Figure 2.

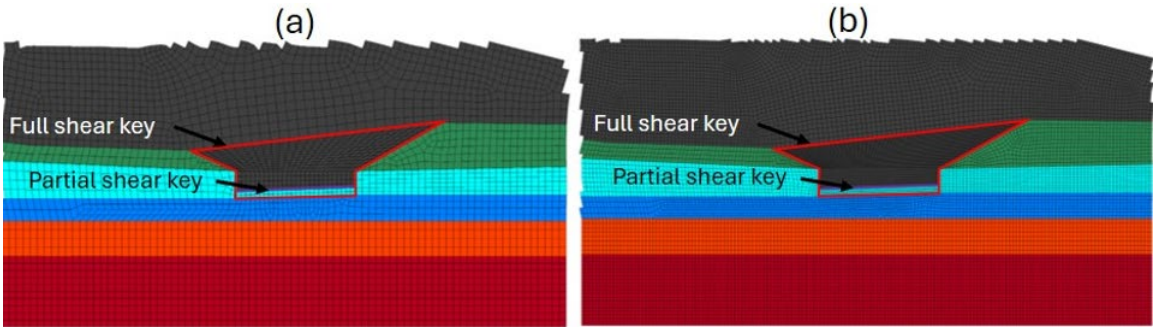


Figure 2: FDM mesh: (a) Maximum element size equal to 0.5; (b) Maximum element size equal to 0.25

For the FDM analyses with remeshing, the entire model geometry was defined as the remeshing domain, with geometry quality checks evaluated every 10 calculation steps using the default FLAC remeshing configuration. For the MPM analyses, the background grid was defined consistently with the finite-difference mesh, while the adopted material point spacing was set equal to the maximum characteristic mesh size (0.5 and 0.25, shown in Figure 3). Additional material point spacing values were internally evaluated; however, the adopted spacing provided stable numerical performance and consistent deformation patterns, and therefore, only these results are presented in this study.

These variations were introduced to investigate their influence on numerical stability, energy dissipation, and the ability of the model to capture deformation localization.

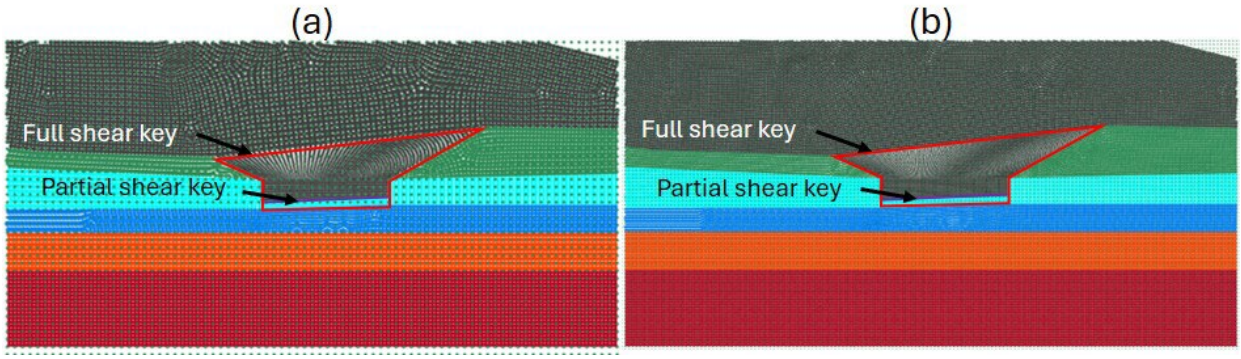


Figure 3: MPM mesh: (a) Maximum element size equal to 0.5; (b) Maximum element size equal to 0.25

Both remeshing and MPoint2D analyses were performed using the large-strain mode (i.e., the grid points move based on the calculated displacement). The analyses were conducted by reducing material strengths from the initial drained condition to either residual or peak undrained strength parameters, depending on the material behavior being represented, as presented in Table 1. The comparison between the remeshing approach and MPoint2D analysis provides a framework for evaluating deformation patterns, runout behavior, and failure mechanism development under large-strain conditions.

Results and Discussion

Table 2 summarizes the results in terms of runout distance and the corresponding FoS obtained from the different numerical approaches. The results are first discussed considering FDM analyses, followed by the MPM simulations.

Table 2: Summary of Runout Distance and FoS

Case	Geometry	Maximum Element Size or Material Point Spacing (m)	Runout Distance (m) / FoS			
			FDM			MPM
			Small-Strain	Large-Strain	Remeshing	MPoint2D
1a	6H:1V with bench, full shear key	0.5	0.26 m / FoS=1.02	0.13 m FoS=1.03	0.13 m FoS=1.03	0.18 m
1b	6H:1V with bench, full shear key	0.25 (refined 2x)	-[1] FoS<1	0.76 m FoS~1	NE[2]	0.44 m
2a	6H:1V with bench, no shear key	0.5	-[1] FoS<1	2.76 m FoS~1	7.2 m FoS~1	2.04 m
2b	6H:1V with bench, no shear key	0.25 (refined 2x)	-[1] FoS<1	>2.32 m^3 FoS <1	9.6 m FoS~1	4.32 m
3a	6H:1V with bench, partial shear key	0.5	-[1] FoS<1	>1.82 m^3 FoS <1	4.25 m FoS~1	0.85 m
3b	6H:1V with bench, partial shear key	0.25 (refined 2x)	-[1] FoS<1	NE[2]	5.92 m FoS~1	3.84 m

Notes:
1. Displacements cannot be calculated because the model is unstable.
2. Not evaluated.
3. Illegal geometries developed during the calculation process, preventing completion of the analysis.

Regarding Case 1, corresponding to the full shear key configuration, the analyses performed using the 0.5 m mesh size showed relatively consistent behavior between the conventional FDM small-strain, FDM large-strain, and remeshing analyses. Under this condition, remeshing was not activated because deformations were relatively low (<0.5 m) and no severe mesh distortion developed. The predicted runout distances obtained for the large-strain analyses (0.13 m) were slightly lower than those obtained from the small-strain analysis (0.26 m), while the calculated FoS values remained close to 1.0 for all analyses. The lower displacements observed in the large-strain simulations are associated with geometric reconfiguration of the downstream slope into a more stable configuration during the analysis.

For the refined mesh case with a maximum element size of 0.25 m, the analyses demonstrated a clear sensitivity to mesh discretization, despite the use of a relatively simple Mohr-Coulomb constitutive model without explicitly modelling the strain-softening behavior. Under small-strain conditions, the calculated FoS was lower (close to 1.0), being unable to converge. The corresponding large-strain analysis predicted a runout distance of approximately 0.76 m. These results highlight the influence of numerical discretization

on stability predictions for conditions approaching marginally stable conditions, where relatively small changes in mesh refinement may significantly affect both FoS and deformation response.

Although the refined mesh analyses produced larger displacements compared to the coarser discretization, the predicted runout distances for Case 1 remained substantially lower than those observed in the subsequent cases involving reduced or partial shear key penetration. This behavior demonstrates the significant stabilizing influence of the shear key in reducing deformation potential within the sensitive foundation layer.

Concerning Case 2, excluding the shear key, the conventional small-strain FDM analyses did not converge for either mesh discretization, indicating unstable conditions when the shear key was removed (FoS<1). A significant mesh influence was also observed in the conventional large-strain analyses. For the 0.5 m element size, the conventional large-strain analysis converged toward a stable condition with a runout distance of approximately 2.76 m and a post-deformation FoS close to unity. In contrast, the refined 0.25 m element size developed illegal geometries during the calculation process, preventing completion of the analysis.

The influence of mesh dependency became more evident when the automatic remeshing was activated. Under remeshing conditions, both mesh discretizations produced comparable runout distances ranging between 7.2 m and 9.6 m, with the larger runout corresponding to the refined mesh. The results indicate that automatic remeshing significantly improves numerical continuity and allows the analyses to capture substantially larger deformation and post-failure runout behavior.

As for Case 3, corresponding to the partial shear key configuration, the analyses produced behavior generally similar to that observed for Case 2. The conventional small-strain FDM analyses did not converge (FoS<1), while the conventional large-strain analyses developed illegal geometries, including the 0.5 m mesh discretization, preventing completion of the simulations. These results indicate increased deformation potential and numerical instability compared to the full shear key configuration under residual undrained strength conditions. The automatic remeshing analyses enabled the calculations to continue despite severe mesh distortion and predicted runout distances of 4.25 m and 5.92 m for the 0.5 m and 0.25 m element-size discretizations, respectively.

The larger runout distances obtained for the refined mesh for Cases 2 and 3 indicate that significant mesh sensitivity remains present even when remeshing techniques are adopted. Nevertheless, both analyses captured similar overall deformation mechanisms and failure patterns. Case 3 (partial shear key configuration) resulted in lower runout distances when compared to Case 2 (no shear key configuration), demonstrating the beneficial influence of partial penetration of the stabilization system into the weak foundation layer. The increase in runout distance observed with mesh refinement suggests that further

discretization studies using smaller element sizes may be warranted to assess the convergence of the predicted deformation response.

Results from the MPoint2D analyses also demonstrated significant sensitivity to material point spacing, with predicted runout distances differing by up to approximately 3 m between the coarse (0.5 m) and fine (0.25 m) discretizations for Cases 2 and 3. The influence of discretization is considered particularly relevant in this case study because the predicted deformation magnitudes are relatively limited, generally below 10 m, making the analyses more sensitive to local strain localization and numerical representation of the failure mechanism.

Additional material point spacing values were internally evaluated; however, several of these analyses developed numerical instability during large deformation. Consequently, the study focused on a comparison between the two primary discretization levels. Further refinement using smaller element sizes, such as 0.125 m, is expected to provide additional insight into discretization effects and shear localization behavior. However, the computational demand associated with the refined analyses was significant, with some simulations requiring more than 48 h of runtime for completion. Additional analyses using finer element sizes were beyond the scope of the present study and will be considered in future work.

Figure 4 and Figure 5 present a comparison of horizontal displacement contours for Case 3 between the remeshing and MPoint2D analyses. Both numerical approaches capture similar deformation patterns; however, the MPoint2D simulation predicts lower displacement magnitudes and reduced runout distances compared to the remeshing formulation.

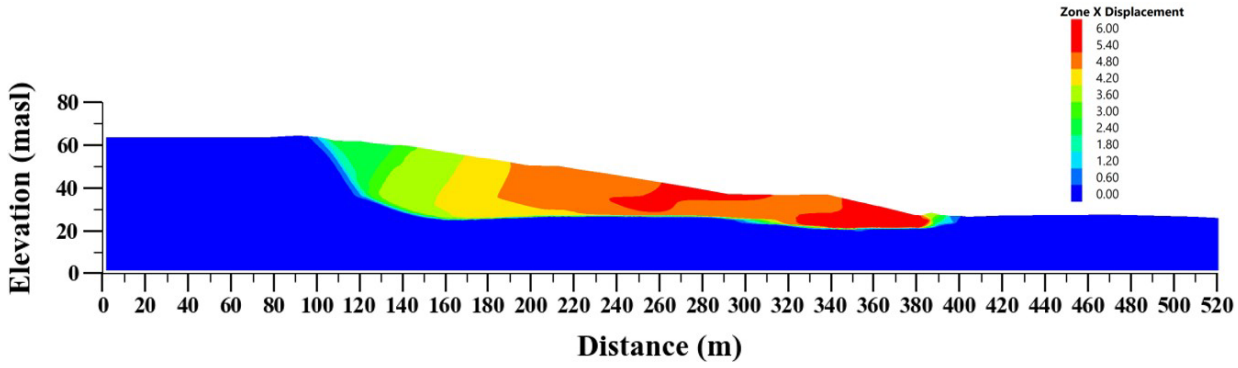


Figure 4: Automatic remeshing results in terms of horizontal displacement – maximum element size = 0.25 m

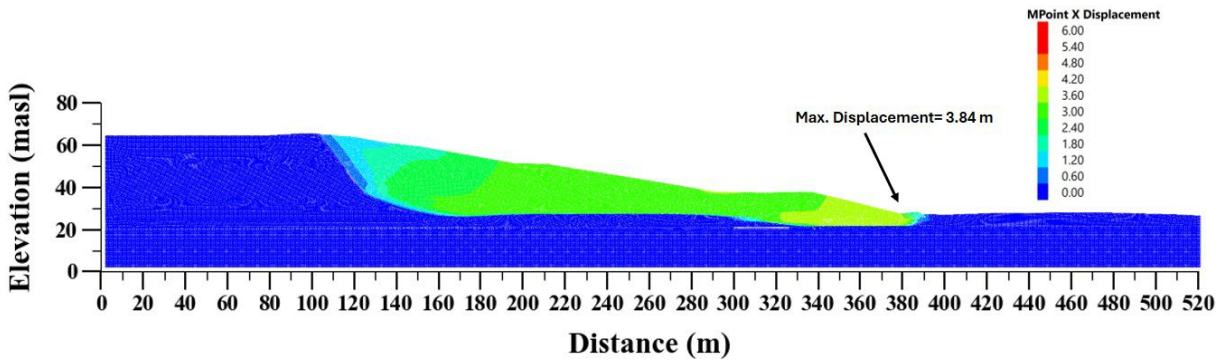


Figure 5: MPM results in terms of horizontal displacement – spacing = 0.25 m

Conclusion

This study presented a comparative assessment of an upstream tailings storage facility (TSF) under residual undrained strength conditions using conventional finite-difference large-strain analyses, remeshing, and MPM (MPoint2D) available within FLAC software. The analyses focused on evaluating deformation magnitude and runout behavior associated with weak and sensitive foundation conditions beneath an interim buttress configuration.

The results demonstrated that conventional small-strain and large-strain finite-difference analyses are highly sensitive to mesh discretization when the factor of safety approaches limiting equilibrium conditions. Even using relatively simple models such as Mohr-Coulomb without explicitly modelling the strain-softening behavior, significant variations in predicted deformation response were observed between the different mesh discretizations. These results support previous observations regarding the importance of mesh dependency and strain localization in residual-strength assessments of TSFs. The analyses also demonstrated the significant influence of the shear key on deformation response. Configurations with complete penetration of the weak foundation layer produced substantially lower runout distances compared to cases with partial or absent shear key penetration. The results highlight the importance of foundation improvement and confinement in controlling deformation magnitude under post-trigger residual undrained strength conditions.

Automatic remeshing significantly improved the ability of the finite-difference analyses to continue after severe mesh distortion developed, allowing evaluation of larger deformation and post-failure runout conditions that could not be captured using conventional large-strain analyses alone. The remeshing formulation produced relatively consistent runout predictions between different mesh discretizations compared to the conventional finite-difference approach. The MPoint2D analyses successfully reproduced the general deformation mechanisms observed in the remeshing simulations while predicting lower displacement magnitudes and runout distances. However, the analyses also demonstrated important

sensitivity to material point spacing, indicating that discretization effects remain a critical consideration even when advanced large-strain numerical approaches are adopted.

In cases where very large deformations are not expected, the remeshing technique can represent a practical and efficient alternative to the MPM, as it is associated with lower computational costs. However, for problems involving large deformations, such as dam-breach analyses where computational demands can become substantial, MPM has emerged as a promising approach and has been applied successfully in a growing number of studies.

Overall, the study demonstrates that deformation-based assessments using large-strain numerical formulations can provide valuable insight into potential post-trigger behavior of TSFs under residual undrained strength conditions. The comparison between automatic remeshing and MPM approaches highlights both the capabilities and current limitations of advanced large-strain numerical methods for evaluating deformation consequences associated with weak foundation conditions and static liquefaction mechanisms in TSFs.

Acknowledgements

The authors gratefully acknowledge the support of Itasca Consulting Group, Minneapolis. The authors also thank Len Murray for reviewing the draft manuscript and his valuable feedback.

References

Itasca Consulting Group, Inc. (2026a). *FLAC2D: Fast Lagrangian analysis of continua in two dimensions* (Version 9.6) [Computer software]. Itasca.

Itasca Consulting Group, Inc. (2026b). *MPoint2D: Material Point Method software for geomechanics* (Beta version; embedded in FLAC 9.7) [Computer software]. Itasca.

Lino, E., Ledesma, O., & Lizcano, A. (2025). Runout analysis using the Material Point Method (MPM) for CDA cases 2A and 2B. In *Proceedings of the Canadian Dam Association (CDA) Annual Conference* (September 29–October 1, 2025).

Macedo, J., Yerro, A., Cornejo, R., & Pierce, I. (2024). Cadia TSF failure assessment considering triggering and posttriggering mechanisms. *Journal of Geotechnical and Geoenvironmental Engineering, 150*(4).

Sulsky, D. L., Chen, Z., & Schreyer, H. (1994). A particle method for history-dependent materials. *Computer Methods in Applied Mechanics and Engineering, 118*, 179–196.

Zabolotnii, E., Morgenstern, N. R., & Wilson, G. W. (2021). Mesh sensitivity in numerical models of strain-weakening systems. *Computers and Geotechnics, 136*, 104253.